

See discussions, stats, and author profiles for this publication at: <https://www.researchgate.net/publication/241503141>

# Characterization of ultrathick photoresists for MEMS applications using a 1X stepper

Article in Proceedings of SPIE - The International Society for Optical Engineering · September 1998

---

CITATIONS

10

READS

803

3 authors, including:



Warren W. Flack

Veeco Inc.

82 PUBLICATIONS 529 CITATIONS

SEE PROFILE

Some of the authors of this publication are also working on these related projects:



E-beam lithography [View project](#)

# Characterization of Ultra-thick Photoresists for MEMS Applications Using a 1X Stepper

Warren W. Flack, Warren P. Fan, Sylvia White  
Ultratech Stepper, Inc.  
San Jose, CA 95134

There is a growing interest in using optical steppers for Micromachining and Microfabrication (MEMS) applications due to the tighter overlay and improved critical dimension (CD) control possible with these lithography tools versus a contact printer or full wafer scanner. MEMS applications frequently require the use of ultra-thick photoresists which can easily exceed fifty microns. Extremely large structure heights and high aspect ratios are often required for micro-electrodeposition of mechanical components such as coils, cantilevers and valves. A stepper has an additional advantage with these structures since the focus can be adjusted at various levels into a thick photoresist, which will result in improved wall angles and enhanced aspect ratios.

The patterning of high aspect ratio structures in these ultra-thick photoresist films is extremely challenging. The aspect ratios easily exceed those encountered in submicron lithography for standard integrated circuit (IC) manufacturing. In addition, the specific photoresist optical properties and develop characteristics degrade the CD control for these ultra-thick films. The bulk absorption effect of the photoresist reduces the effective dose at the bottom of the film. This effect is exacerbated by the isotropic wet development process, which produces sloped profiles. Unlike thin photoresist for IC manufacturing, lithography modeling and characterization tools are not available for ultra-thick photoresist films.

For this study the performance of several commercially available positive and negative ultra-thick photoresists is examined at a thickness of fifty microns using both high throughput i-line and gh-line lithography systems optimized for thick photoresist processing. The photoresists used in this study are selected to represent the full range of available chemistries available from different suppliers. Basic photoresist characterization techniques created for thin films are applied to the ultra-thick photoresist films. Cross sectional SEM analysis, process linearity and Bossung plots are used to establish relative lithographic capabilities of each photoresist. The trade-offs between the various photoresist chemistries are reviewed and compared with the process requirements for high aspect ratio applications.

**Key Words:** ultra-thick photoresist, MEMS, photoresist characterization, resolution

## 1.0 INTRODUCTION

It is anticipated that the MEMS market will continue to expand into various markets such as medical devices including single use health monitors, automotive applications such as airbag actuators, accelerometers for braking and suspension systems and many other micromachined products such as motors, nozzles, valves, pumps, micromirror structures and sensors [1]. With this level of growth will come an increased need for ultra-thick photoresist films due to the extremely large structure heights that are often required to form these devices. In semiconductor applications a photoresist film thickness of less than 2  $\mu\text{m}$  is typically required for ion implantation or etch procedures but for MEMS applications, photoresist thickness can actually exceed 1000  $\mu\text{m}$  depending upon the application [2]. While

thin film photoresists have been well characterized and modeled, this information may not adequately describe the performance of thicker photoresist films. The use of ultra-thick photoresist films creates a new set of lithographic challenges [3, 4].

In some applications ultra-thick photoresist is used as a mold, for example, in the formation of bond pads for bump bond applications [5, 6]. The photoresist which may be 50 or 100  $\mu\text{m}$  thick needs to be patterned to act as a mold for these devices. This pattern in thick photoresist may need to have a high aspect ratio depending upon the type of structure. There are a number of challenges in imaging thick photoresist which can make it difficult to obtain a small CD. This can be visualized by considering that a CD of 10  $\mu\text{m}$  in a thick 50  $\mu\text{m}$  photoresist has an aspect ratio that would be equivalent to a 0.2  $\mu\text{m}$  line in 1.0  $\mu\text{m}$  of photoresist.

One popular MEMS technique is to use a sacrificial layer such as silicon dioxide, metal or photoresist as a mold which is subsequently electroplated with metal or deposited with a film (LIGA) [7]. The sacrificial layer is then removed to release the microstructure to form-free-standing structures. For some MEMS applications there may be multiple sacrificial layers which are developed and plated in turn to form step like microstructures [7, 8, 9, 10]. Innumerable devices can be produced using this technique. LIGA typically requires extra lithography and etch steps to pattern the dielectric or metal layer. These applications often utilize a thick photoresist layer to protect the substrate during etching of silicon dioxide or metal layers. This layer must often be quite thick because of the harsh etch conditions required to pattern these layers.

There are a number of drawbacks to using LIGA molds including the number of additional processing steps and the associated expense. Because of these difficulties there is increasing interest in the use of photoresist as the sacrificial layer [2, 7, 8, 9, 10, 11, 12, 13]. The use of photoresist as the sacrificial layer would significantly reduce the number of processing steps required to produce the molds for various microstructures. This may not be suitable for every application, however, due to the photoresist process limitations.

Because of the growing need for improved overlay and CD in MEMS applications there is wide interest in utilizing steppers. A stepper offers tighter overlay and improved CD in comparison to a contact printer or full wafer scanner. In addition, stepper systems can adjust the focus into a thick photoresist which will result in improved wall angles and better aspect ratios as compared to other lithography tools. Ultra-thick photoresists typically require a large exposure dosage for high aspect ratio lithography. For this reason, it is advantageous to utilize a stepper with a broad band exposure system to maximize the illumination intensity at the wafer plane. Another consideration is the stepper alignment system. It is advantageous to have a flexible alignment system that eliminates the requirement for dedicated alignment targets on the wafer. A pattern recognition based alignment system has the flexibility to align to marks already present on the substrate [14].

Several commercially available photoresists representing a range of available chemistries were chosen for examination in this paper. The photoresists chosen include novalac based AZ-9260, polyhydroxy styrene based Futurrex, acryl based JSR THB-30MB and epoxy based SU8. Except for the AZ-9260, all photoresists are negative acting. Several of these photoresists are broadband or deep UV sensitive materials. Because of this, both i-line and gh-line steppers were used to evaluate the various photoresist materials.

## 2.0 EXPERIMENTAL METHODS

### 2.1 Reticle Design and Manufacture

The Ultratech 1X reticle used for this study was designed primarily to support easy cross sectional SEM metrology for MEMS applications. The reticle consists of two 55 by 25 mm fields, one of each polarity to support both positive and

negative acting photoresists. Each field contains horizontal and vertical grouped line and space patterns from 2 to 20  $\mu\text{m}$  in 1  $\mu\text{m}$  size increments, and from 22 to 44  $\mu\text{m}$  in 2  $\mu\text{m}$  size increments. The length of the line and space pairs are designed to facilitate cross sectional SEM analysis. The reticle was written on a MEBES 4500 using a high resolution PBS resist. There was no data biasing applied to the design data and CDs were held to within  $\pm 0.03 \mu\text{m}$  of a nominal 2.0  $\mu\text{m}$  chrome line. Reticle CD information was also obtained for all line sizes on both fields to establish the process linearity in reticle fabrication.

## 2.2 Lithography Equipment

Lithography for each photoresist evaluated in this study was performed on either an Ultratech Stepper Saturn Wafer Stepper<sup>®</sup> or Ultratech Stepper Titan Wafer Stepper<sup>®</sup> depending upon its optimal spectral sensitivity. The Saturn stepper and the Titan stepper are based on the 1X Wynne-Dyson lens design employing Hg broadband i-line illumination from 355 to 375 nm (Saturn), or the Hg broadband gh-line illumination from 390 to 450 nm (Titan) [15]. The specifications of both lithography systems used in this study are shown in Table 1. Both steppers use Machine Vision System (MVS), a pattern recognition system, to align to structures already present on a substrate. Exposure uniformity was verified prior to collecting the experimental data and was found to be 1.2 percent across the entire field. Multiple wafers were exposed with a layout consisting of a seven by seven field array as illustrated in Figure 1. Nominal exposure dose was determined by measuring line and space patterns at the specific linewidth of interest with a Hitachi S-7280H metrology SEM. A 50 percent threshold criteria was selected for the determination of the linewidth CD for both the negative and positive photoresists.

## 2.3 Processing Conditions

SEMI standard ultra-flat silicon wafers were used for this study. The 150 mm wafers were pre-treated according to recommendations by the photoresist manufacturers as described in process Tables 2, 3, 4 and 5. Four commercially available ultra-thick photoresist products were used for this investigation: AZ-9260<sup>®</sup> positive photoresist, NR5-8000<sup>®</sup> negative photoresist, THB-30MB<sup>®</sup> negative photoresist, and SU8-5<sup>®</sup> negative photoresist. The AZ-9260 is manufactured by the AZ-Clariant Corporation. THB-30MB is manufactured by Japanese Synthetic Rubber company (JSR). NR5-8000 is manufactured by Futurrex Inc., and SU8-5 is manufactured by Microlithography Chemical Corporation (MCC). These photoresists were selected because of the diversity of their photo-chemistries as discussed in Section 3.0. Each photoresist was coated to the 50  $\mu\text{m}$  target thickness using the process and equipment described in Tables 2, 3, 4 and 5. Photoresist thickness and uniformity were measured on a Dektak 3030 surface profilometer measurement system. Note that the three negative photoresists were coated with a single coating step while the AZ-9260 required three coatings to achieve the desired photoresist thickness.

## 2.4 Data Analysis

Wafers coated with each of the four photoresists were exposed on either the gh-line or the i-line lithography system based on optimal spectral sensitivity of the individual photoresist. Each wafer was visually inspected and measured on the Hitachi S-7280H SEM to determine the photoresist linearity over a range of linesizes. CD measurements were taken at 20.0Kx magnification whereas SEM micrographs were taken at 1.30Kx magnification. The two smallest line sizes within a 10 percent linearity window were then measured on the S-7280H over the entire focus and exposure matrix as illustrated in Figure 1. This CD data was used to generate Bossung plots for each photoresist. A 10 percent CD process control window was calculated from the Bossung plot. SEM micrographs are presented to illustrate masking linearity in dense lines/spaces. The CD linearity data is also plotted for each photoresist. The results from the data analysis are discussed in Section 3.0.

### 3.0 RESULTS AND DISCUSSIONS

#### 3.1 Clariant AZ-9260

Clariant AZ-9260 is a positive, novolac-based, broad spectral sensitivity photoresist. Its lithographic performance was initially evaluated on the i-line Saturn stepper. The dose-to-clear ( $E_0$ ) was determined to be in excess of  $5000 \text{ mJ/cm}^2$  and therefore the i-line evaluation was dropped. Its lithographic performance on the gh-line Titan stepper was then evaluated and found to provide a substantially lower  $E_0$  value. Cross sectional SEM micrographs of AZ-9260 on the Titan are shown in Figure 2a. Here the mask linearity for  $50 \mu\text{m}$  thick AZ-9260 photoresist are illustrated for CD ranges of  $30 \mu\text{m}$  to  $7 \mu\text{m}$  at an exposure energy of  $3050 \text{ mJ/cm}^2$  and a focus offset of  $-19 \mu\text{m}$ .

Clariant AZ-9260 demonstrated an  $8 \mu\text{m}$  resolution for dense lines and spaces in the gh-line as shown in Figure 2a. However, the resolved  $8 \mu\text{m}$  line resolution may not be functional in practical applications due to the sloped foot observed at the base of the photoresist. The footage becomes more pronounced as the line size decreases. The resolution appears to be limited to approximately  $11 \mu\text{m}$  for applications requiring plating. A bulging shape near the top of the photoresist was observed and is characteristic of this material. The bulging shape is caused by a combination of softbake temperature, surface inhibition and multiple bakings.

Figure 2b shows the mask linearity plot for Clariant AZ-9260 photoresist at an exposure dose of  $3050 \text{ mJ/cm}^2$  and a focus offset of  $-19 \mu\text{m}$ . The dashed lines show  $\pm 10$  percent control limits for the linewidth. The optimal reticle bias was determined to be  $-2.1 \mu\text{m}$  by regression analysis. Of the four photoresists evaluated in this study, AZ-9260 exhibits the best mask linearity. This result is expected since the other photoresists are negative acting.

Figure 2c shows two Bossung plots generated through a focus and exposure matrix for AZ-9260 for both the  $9 \mu\text{m}$  and the  $11 \mu\text{m}$  nominal CDs. The Clariant AZ-9260 shows no significant variability in CD as a function of focus offset for either linesize. However, the CD variation in terms of exposure doses is more pronounced. The Bossung plot of the  $9 \mu\text{m}$  mask CD shows that higher exposure doses tend to fall within the  $12 \mu\text{m}$  focus window, which indicates that the film thickness does play an important role in photoresist performance. The CD starts to fall completely outside of the  $+10$  percent control limit at the lower doses, which corresponds to a 5 percent exposure latitude for the  $9 \mu\text{m}$  mask CD. For the  $11 \mu\text{m}$  mask CD plot, the CD begins to fall outside the  $+10$  percent control limit around  $-11 \mu\text{m}$  focus, which corresponds to an 8 percent exposure latitude and a total depth of focus (DOF) of  $8 \mu\text{m}$ . The Bossung plots confirm the bias of  $-2.1 \mu\text{m}$  determined by the linearity regression analysis. To use the Bossung plots to determine a more accurate focus latitude, the focus window would need to be extended beyond the  $12 \mu\text{m}$  range used in this study.

#### 3.2 Futurrex NR5-8000

Futurrex NR5-8000 is a negative, polyhydroxy-styrene based photoresist designed for i-line applications. It uses an aqueous, TMAH based developer. Its lithographic performance on the i-line Saturn stepper was evaluated in this study. Wafers were imaged on the Saturn stepper with exposure energies varying from  $900 \text{ mJ/cm}^2$  to  $1200 \text{ mJ/cm}^2$  and the focus offsets varied from  $-19 \mu\text{m}$  to  $-7 \mu\text{m}$ . Cross sectional SEM micrographs are shown in Figure 3a. Futurrex NR5-8000 demonstrated  $9 \mu\text{m}$  resolution for dense lines and spaces. The side wall angles for the resolved features were calculated to be better than 88 degrees for the range of line sizes resolved based on cross sectional SEM measurements of the top and bottom spacewidths. No curvature or foot was observed at the base of the photoresist. The photoresist residue observed for small linewidths using the other negative photoresists is not observed here.

Figure 3b shows the mask linearity plot for NR5-8000 photoresist with an exposure dose of  $1100 \text{ mJ/cm}^2$  and a focus offset of  $-15 \mu\text{m}$ . The dashed lines show  $\pm 10$  percent control limits for the linewidth. NR5-8000 exhibits a mask linearity down to  $9 \mu\text{m}$  nominal linewidth with a reticle bias of  $+1.7 \mu\text{m}$  as determined by regression analysis.

Figure 3c shows two Bossung plots generated through a focus and exposure matrix for NR5-8000 for both 9  $\mu\text{m}$  and 11  $\mu\text{m}$  nominal CDs. The Bossung plot generated for the 9  $\mu\text{m}$  feature size shows that the CD starts to fall outside the +10 percent control limits at -15  $\mu\text{m}$  focus offset which yields approximately 17 percent in exposure latitude and 8  $\mu\text{m}$  DOF. In contrast, the Bossung plot generated for the 11  $\mu\text{m}$  feature size shows a wider focus window. The CD starts to fall outside the +10 percent control limits at -17  $\mu\text{m}$  focus offset which provides approximately 17 percent in exposure latitude and 10  $\mu\text{m}$  DOF. The Bossung plots validate the 1.7  $\mu\text{m}$  positive bias determined from the mask linearity plot. To explore the full range of DOF, the focus window must be extended beyond the 12  $\mu\text{m}$  range used in this study.

Figure 3d shows the normalized film retention curve for the negative Futurrex NR5-8000 photoresist. The after develop film thickness was measured at -15  $\mu\text{m}$  defocus over the full range of exposure doses used. A value of 1 indicates that the film thickness is the same as the pre-develop thickness. An average value of 0.95 is measured over the exposure doses used for this study, which indicates excellent film retention.

### 3.3 JSR THB-30MB

JSR THB-30MB is a negative, acryl-based photoresist designed for broad band spectrum applications. It uses an aqueous TMAH based developer. Its lithographic performance on both the i-line Saturn stepper and the gh-line Titan stepper was previously evaluated at a film thickness of 25  $\mu\text{m}$  [16]. In that study, the JSR THB series negative photoresist demonstrated a resolution of 8  $\mu\text{m}$  in i-line and 20  $\mu\text{m}$  in gh-line. Based on these results, the i-line Saturn stepper was chosen for a continued evaluation of this photoresist at a 50  $\mu\text{m}$  film thickness.

Cross sectional SEM micrographs of JSR THB-30MB are shown in Figure 4a at an exposure energy of 1750  $\text{mJ}/\text{cm}^2$  and -15  $\mu\text{m}$  focus offset. JSR THB-30MB demonstrated a 13  $\mu\text{m}$  resolution for dense lines and spaces in the i-line shown in Figure 4a. A slight curvature at the foot is observed at the base of the photoresist across the feature sizes evaluated. The observed footage becomes more pronounced as the line size decreases. The side wall angles for the 13  $\mu\text{m}$  line were calculated to be better than 88 degrees based on cross section SEM measurements of the top and bottom spacewidths. A photoresist residue is observed here at line sizes 13  $\mu\text{m}$  and below. A proposed mechanism for this phenomena is described in Section 3.4. Under these conditions, 14  $\mu\text{m}$  dense lines and spaces should be considered as the minimum practical resolution for the JSR THB-30MB.

Figure 4b shows the mask linearity plot for JSR THB-30MB photoresist at the exposure dose of 1750  $\text{mJ}/\text{cm}^2$  and the focus offset of -15  $\mu\text{m}$ . The dashed lines show  $\pm 10$  percent control limits for the linewidth. Clearly the linearity plot shows a discontinuity between the 20  $\mu\text{m}$  to 22  $\mu\text{m}$  nominal linewidth which degrades the linearity. The ultimate linearity starts to fail at about 13  $\mu\text{m}$ . A reticle bias of +2.1  $\mu\text{m}$  was determined by regression analysis.

Figure 4c shows two Bossung plots generated through the focus and exposure matrix for THB-30MB exposed at i-line. The Bossung plot generated for the 13  $\mu\text{m}$  feature shows that the CD starts to fall outside the +10 percent control limits at -14  $\mu\text{m}$  focus offset which yields approximately 10 percent in exposure latitude and 7  $\mu\text{m}$  DOF. The Bossung plot generated for the 15  $\mu\text{m}$  feature shows a wider DOF. Here, CD starts to fall outside the +10 percent control limits at -17  $\mu\text{m}$  focus offset which yields approximately 20 percent in exposure latitude and 10  $\mu\text{m}$  DOF. The Bossung plots show a larger bias than the +2.1  $\mu\text{m}$  bias determined by the regression analysis because of the poor linearity in Figure 4b. To use the Bossung plots to determine a more accurate focus latitude, the focus window would need to be extended further in the positive focus offset direction.

Figure 4d shows the normalized film retention curve. The after develop film thickness was measured at -14  $\mu\text{m}$  focus offset over the full range of exposure doses used in the study. A value of 1 indicates that the film thickness is the same as the pre-develop thickness. An average value of 0.90 is measured over the exposure doses used in this study, which indicates excellent film retention.

### 3.4 MCC SU8-5

MCC SU8-5 is a negative, epoxy-type, Shell Chemical EPON<sup>®</sup> resin based photoresist. Previous evaluation of SU8-5 on the Titan stepper showed minimal photo-sensitivity in the g-line spectrum [16]. Therefore, the Saturn was chosen for continuing evaluation of this photoresist at 50  $\mu\text{m}$  thickness. Wafers were imaged on the Saturn stepper with exposure energies varying from 400  $\text{mJ}/\text{cm}^2$  to 550  $\text{mJ}/\text{cm}^2$  and focus offsets varying from -19  $\mu\text{m}$  to -7  $\mu\text{m}$ . SU8-5 demonstrated an 8  $\mu\text{m}$  resolution for dense lines and spaces in the i-line as illustrated by the cross sectional SEM micrographs shown in Figure 5a. The side wall angle for the resolved 8  $\mu\text{m}$  line was calculated to be better than 88 degrees based on cross section SEM measurements of the top and bottom linewidths. No curvature or foot was observed at the base of the photoresist.

An interesting residue phenomena was observed for the 7  $\mu\text{m}$  dense lines and spaces as shown in Figure 5a. Here the bottom 80 percent of the photoresist lines were cleared, yet the remaining 20 percent of the photoresist has residue accumulated near the top. Figure 6 shows a top-down view where a bubble formation is clearly visible. One postulated hypothesis for such phenomena is a sensitizer “snowplow” effect. This describes a situation where the prebake drives the photosensitizer along with the residual solvent toward the top of the un-exposed area where it accumulates as the diffusion decreases toward the end of the bake cycle. This highly concentrated band of sensitizer is then extremely sensitive to any stray light during the exposure process. This is an interesting phenomenon because it appears to limit the ultimate photoresist performance in terms of resolution. The “snowplow” effect is also observed for the JSR THB-30MB photoresist which suggests that it may be a common issue with certain types of negative acting chemistries.

Figure 5b shows the mask linearity plot for SU8-5 photoresist where an exposure dose of 400  $\text{mJ}/\text{cm}^2$  and a focus offset of -13  $\mu\text{m}$  were used. The dashed lines show  $\pm 10$  percent control limits for the linewidth. SU8-5 exhibits excellent mask linearity for a negative photoresist. An optimal reticle bias of +3.0  $\mu\text{m}$  was determined by regression analysis.

Figures 5c shows two Bossung plots generated through a focus and exposure matrix for SU8-5 exposed at i-line. The SU8-5 shows no significant variability in CD as a function of focus offset for both the 8  $\mu\text{m}$  and the 10  $\mu\text{m}$  nominal CDs. The lower exposure doses show a reasonably flat CD response across the focus range and all of the CD measurements except at the highest doses are within the  $\pm 10$  percent of the nominal CD limits. It appears that the total DOF for both the 8  $\mu\text{m}$  and the 10  $\mu\text{m}$  lines exceeds the 12  $\mu\text{m}$  focus window chosen for this study. The Bossung plots confirm the 3.0  $\mu\text{m}$  positive bias from the mask linearity plot. From the Bossung plot, it can be seen that a 25 percent exposure latitude is observed for the 8  $\mu\text{m}$  mask CD and a 30 percent exposure latitude for the 11  $\mu\text{m}$  mask CD. To use the Bossung plots to determine optimum DOF, the focus window would need to be extended in both focus directions.

Figure 5d shows the normalized film retention curve for the negative acting SU8-5 photoresist. The after develop film thickness was measured at -15  $\mu\text{m}$  defocus over a range of exposure doses. A value of 1 indicates that the film thickness is the same as the pre-develop thickness. An average value of 0.90 was measured over the exposure doses used in this study which indicates excellent film retention.

## 4.0 CONCLUSIONS

Standard photoresist characterization techniques have been applied to four commercially available thick photoresist products, Clariant AZ-9260, JSR THB-30MB, Futurrex NR5-8000 and MCC SU8-5. Cross sectional SEM analysis and Bossung plots were used to establish relative lithographic capabilities of each photoresist. The trade-offs between the various photoresist chemistries were reviewed and compared with the process requirements for MEMS applications.

A summary of recommended lithographic applications for the four photoresist products is given in Table 6. It is clear that the NR5-8000 and SU8-5 offer the best resolution of the four photoresists. The SU-8 has the lowest dose, which is an advantage for stepper throughput and overall cost-of-ownership. The AZ-9260 demonstrated the best linearity, but has the disadvantage of the highest nominal exposure dose of the four photoresists studied.

This paper has explored the performance of all four photoresists for high-aspect-ratio MEMS applications on Ultratech Saturn and Titan family steppers. Aspect ratios in excess of 7 to 1 were demonstrated in 50  $\mu\text{m}$  film thicknesses. A future paper will discuss the capabilities of these photoresists at 100  $\mu\text{m}$  film thicknesses.

## 5.0 REFERENCES

1. Marshall, "MEMS Technologies - On the Brink of Maturity?" *R & D Magazine*, July 1997.
2. Lorenz, "High-Aspect-Ratio, Ultrathick, Negative-Tone Near-UV Photoresist and Its Applications for MEMS," *Sensors and Actuators*, A64 (1), January 1998.
3. Flores, Flack, Tai, "An Investigation of the Properties of Thick Photoresist Films," *Advances in Resist Technology and Processing XI Proceedings*, SPIE 2195, 1994.
4. Flores, Flack, Tai, Mack "Lithographic Performance in Thick Photoresist Applications," *OCG Microlithography Seminar*, Interface '93 Proceedings, 1993.
5. Cheang, Staud, Newman, "A Low Cost Lithography Process for Flip Chip Applications in Advanced Packaging Industry," *Advanced Manufacturing Technologies Seminar*, 1997.
6. Lau, "Next Generation Low Cost Flip Chip Technologies," *46th Electronic Components & Technology Conference*, 1996.
7. Conedera, Fabre, Dilhan, "A Simple Optical System to Optimize a High Depth to Width Aspect Ratio Applied to a Positive Photoresist Lithography Process," *Journal of Micromechanics and Microengineering*, 7(3), September 1997.
8. Cui, Lawes, "A New Sacrificial Layer Process for the Fabrication of Micromechanical Systems," *Journal of Micromechanics and Microengineering*, 7(3), September 1997.
9. Lehr, "New Extensions of LIGA Technology," *Micromachine Devices*, November 1996.
10. Guerin, "Simple and Low Cost Fabrication of Embedded Micro-Channels by Using A New Thick-Film Photoplastic," *International Conference on Solid State Sensors and Actuators*, Volume 1, 1997.
11. LaBianca, "High Aspect Ratio Resist for Thick Film Applications," *Advances in Resist Technology and Processing XII Proceedings*, SPIE 2438, 1995.
12. Lorenz, "SU-8: A Low Cost Negative Resist for MEMS," *Journal of Micromechanics and Microengineering*, 7(3), 1997.
13. Dellman, "Fabrication Process of High Aspect Ratio Elastic Structures for Piezoelectric Motor Applications," *International Conference on Solid State Sensors and Actuators*, Volume 1, 1997.
14. Flack, Flores, Tran, "Application of Pattern Recognition in Mix-and-Match Lithography," *Optical/Laser Microlithography VIII Proceedings*, SPIE 2440, 1995.
15. Flores, Flack, Dwyer, "Lithographic Performance of a New Generation i-line Optical System," *Optical/Laser Lithography VI Proceedings*, SPIE 1927, 1993.

16. Flack, Fan, White, "The Optimization and Characterization of Ultra-thick Photoresist Films," *Advances in Resist Technology and Processing XV Proceedings*, SPIE 3333, 1998.

Parameter	Titan	Saturn
Reduction factor	1X	1X
Wavelength (nm)	390-450	355-375
Numerical aperture (NA)	0.32	0.365
Partial coherence ( $\sigma$ )	0.50	0.44
Wafer plane irradiance (mW/cm <sup>2</sup> )	1200	700

Table 1: Specifications of the lithography systems used in this study.

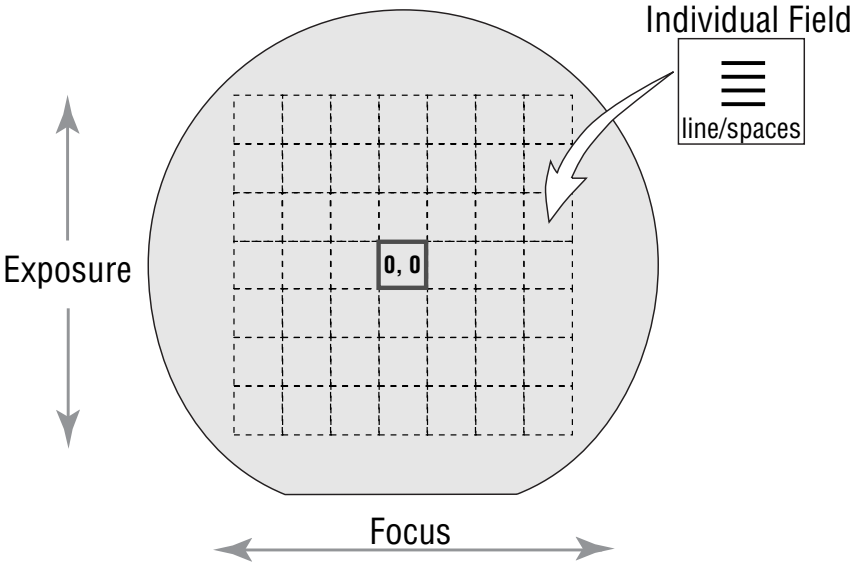


Figure 1: Wafer layout for the focus and exposure test matrix.

Process Step	Parameters	Equipment
Adhesion Promotion	HMDS vapor prime	YES LP-3 Oven
Photoresist Coat-1	Static dispense: 0 rpm for 15 seconds Spread: 300 rpm for 3 seconds Spin: 1700 rpm for 60 seconds Spin: 500 rpm for 10 seconds Spin dry: 1000 rpm for 10 seconds	MTI
Softbake-1	10 seconds at 110°C, 0.001 gap 80 seconds at 110°C, full contact	MTI
Photoresist Coat-2, 3	Static dispense: 0 rpm for 15 seconds Spread: 300 rpm for 3 seconds Spin: 1000 rpm for 60 seconds Spin: 500 rpm for 10 seconds Spin dry: 1000 rpm for 10 seconds	MTI
Softbake-2, 3	10 seconds at 110°C, 0.001 gap 160 seconds at 110°C, full contact	MTI
Develop	AZ400K (1:4) at 21°C Puddle: 600 seconds total with puddle renewals every 120 seconds	Batch
Rinse	DI water rinse for 30 seconds then gently air dry	Batch

Table 2: Process conditions for Clariant AZ-9260 photoresist.

Process Step	Parameters	Equipment
Photoresist Coat	Static dispense: 0 rpm for 10 seconds Spread: 1250 rpm for 10 seconds Spin: 380 rpm for 1 second	MTI
Softbake	120 seconds at 110°C, 0.010-inch proximity 20 minutes at 110°C, full contact	MTI
PEB	60 seconds at 100°C	Solitec VBS-200
Develop	RD5 developer at 21°C 270 seconds immersion with continuous agitation	Batch
Rinse	DI water rinse for 60 seconds then gentle air dry	Batch

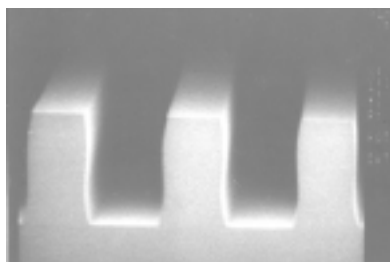
Table 3: Process conditions for Futurrex NR5-8000 photoresist.

Process Step	Parameters	Equipment
Adhesion Promotion	HMDS vapor prime	YES LP-3 Oven
Photoresist Coat	Static dispense: 0 rpm for 10 seconds Spread: 1250 rpm for 10 seconds Spin: 3000 rpm for 1 second	Solitec 5110C Coater
Softbake	300 seconds at 90°C, hard-contact	Solitec VBS-200
Develop	Diluted PD523AD (0.5% TMAH) at 21°C Puddle: 720 seconds total with puddle renewals every 120 seconds	Batch
Rinse	DI water rinse for 60 seconds oven dried, vertical orientation for 40 seconds	Batch

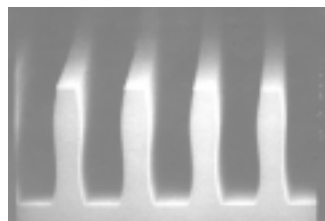
Table 4: Process conditions for JSR THB-30MB photoresist.

Process Step	Parameters	Equipment
Wafer Preparation	Bake at 200°C for 15 minutes	YES LP-3 Oven
Photoresist Coat	Static dispense: 0 rpm for 10 seconds Spin: 490 rpm with 5 seconds ramp and 400 rpm 15 seconds hold	Solitec 5110C Coater
Softbake	300 seconds at 68°C, hard-contact then 900 seconds at 90°C, hard-contact	Solitec VBS-200
Post Exposure Bake	60 seconds at 50°C, then 60 seconds at 90°C	Solitec VBS-200
Develop	SU8-5 developer at 21°C 180 seconds immersion with mild agitation then 420 seconds stagnant immersion	Batch
Rinse	Rinse with SU8-5 developer for 30 seconds then gently air dry	Batch

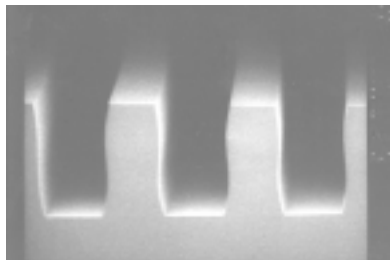
Table 5: Process conditions for MCC SU8-5 photoresist.



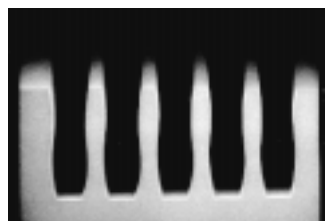
Mask = 30.0  $\mu\text{m}$  line/space



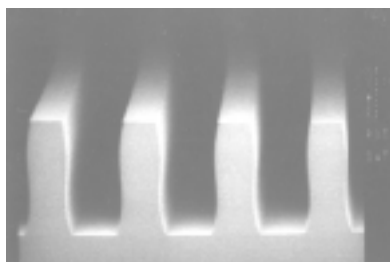
Mask = 14.0  $\mu\text{m}$  line/space



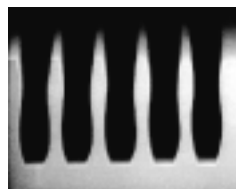
Mask = 26.0  $\mu\text{m}$  line/space



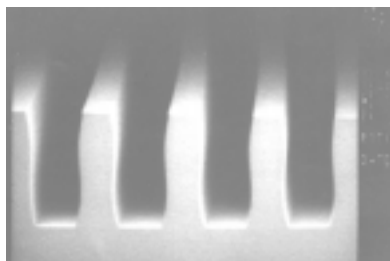
Mask = 11.0  $\mu\text{m}$  line/space



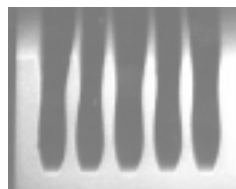
Mask = 20.0  $\mu\text{m}$  line/space



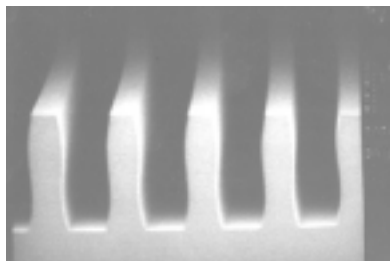
Mask = 9.0  $\mu\text{m}$  line/space



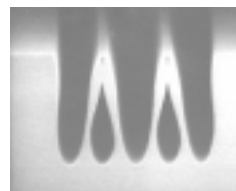
Mask = 18.0  $\mu\text{m}$  line/space



Mask = 8.0  $\mu\text{m}$  line/space



Mask = 16.0  $\mu\text{m}$  line/space



Mask = 7.0  $\mu\text{m}$  line/space

**Figure 2a:** Mask linearity for 50  $\mu\text{m}$  thick Clariant AZ-9260 photoresist. The exposure dose is 3050  $\text{mJ}/\text{cm}^2$  and the focus offset is -19  $\mu\text{m}$ .

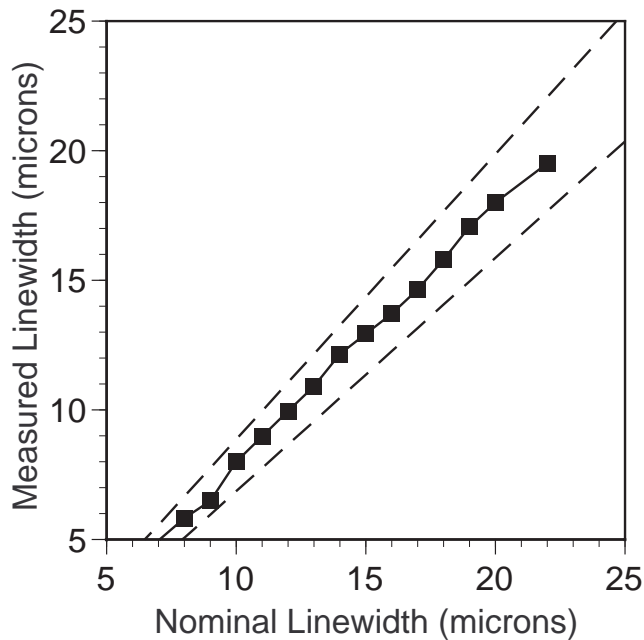


**Figure 2b:** Mask linearity plot for Clariant AZ-9260 photoresist. The exposure dose is 3050 mJ/cm<sup>2</sup> and the focus offset is -19 μm. The dashed lines show ±10 percent control limits for the linewidth. A reticle bias of -2.1 μm was determined by regression analysis.

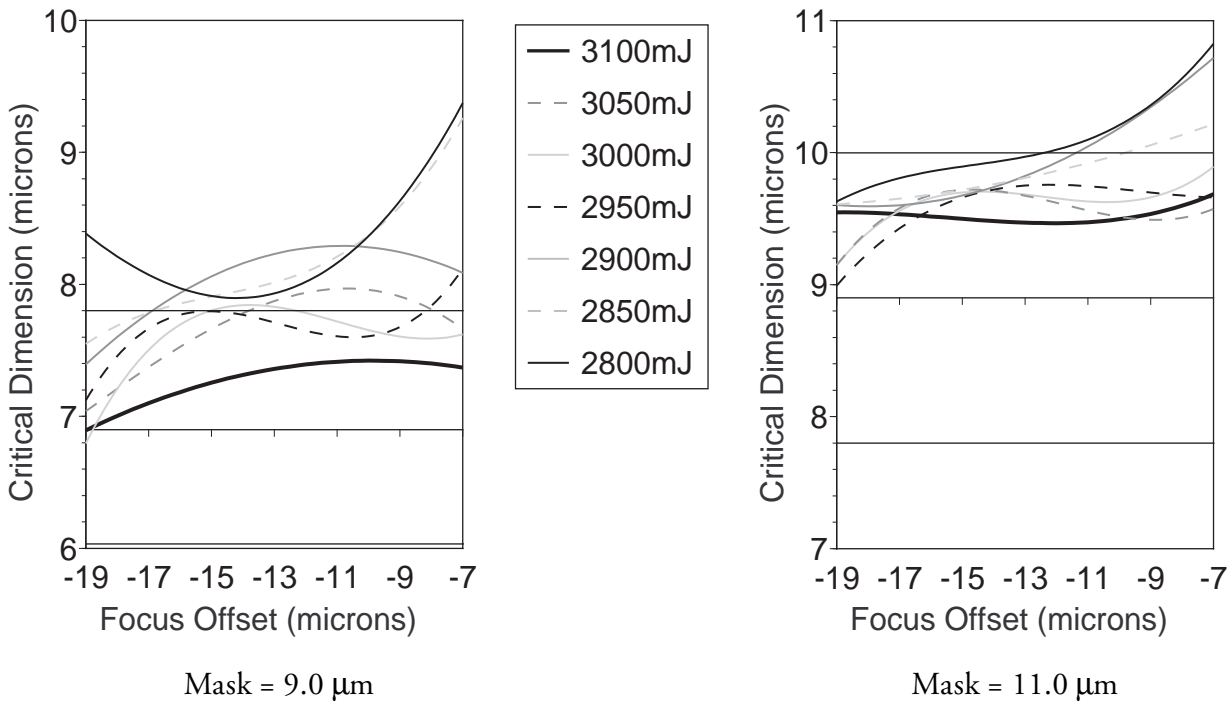
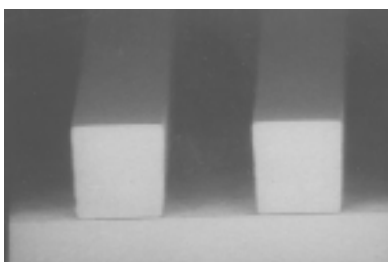
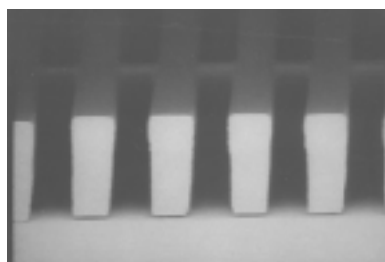


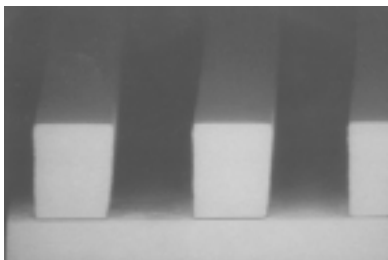
**Figure 2c:** Focus and exposure matrix for Clariant AZ-9260 photoresist exposed at gh-line. The horizontal lines show ±10 percent control limits based on the photomask size. The nominal photoresist size is biased by -2.1 μm based on the photomask linearity.



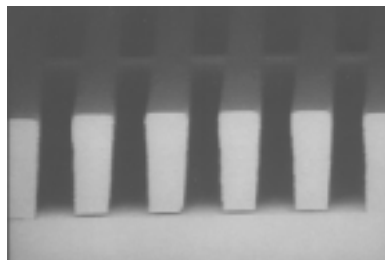
Mask = 30.0  $\mu\text{m}$  line/space



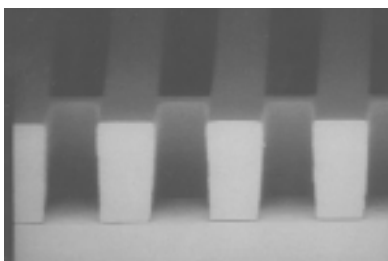
Mask = 13.0  $\mu\text{m}$  line/space



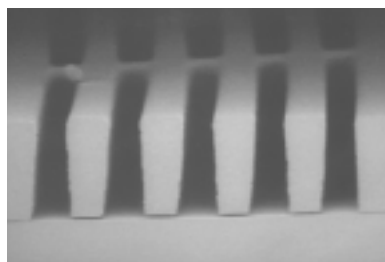
Mask = 26.0  $\mu\text{m}$  line/space



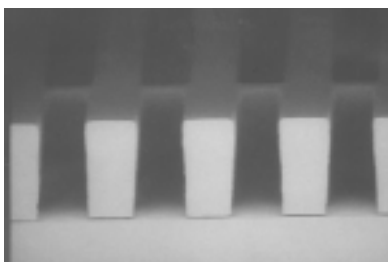
Mask = 12.0  $\mu\text{m}$  line/space



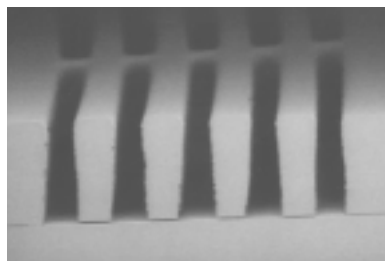
Mask = 18.0  $\mu\text{m}$  line/space



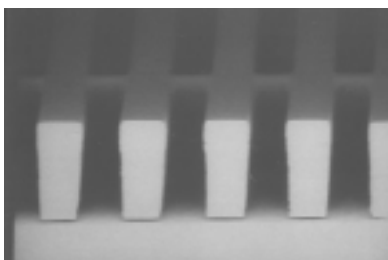
Mask = 11.0  $\mu\text{m}$  line/space



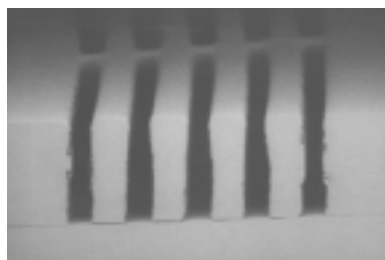
Mask = 16.0  $\mu\text{m}$  line/space



Mask = 10.0  $\mu\text{m}$  line/space



Mask = 14.0  $\mu\text{m}$  line/space



Mask = 9.0  $\mu\text{m}$  line/space

**Figure 3a:** Mask linearity for 50  $\mu\text{m}$  thick Futurrex NR5-8000 photoresist. The exposure dose is 1100  $\text{mJ}/\text{cm}^2$  and the focus offset is -15  $\mu\text{m}$ .

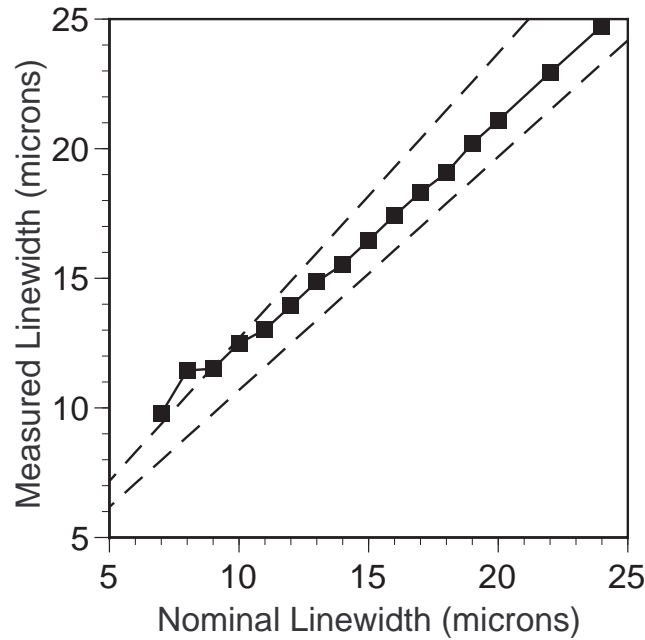


**Figure 3b:** Mask linearity plot for Futurrex NR5-8000 photoresist. The exposure dose is 1100 mJ/cm<sup>2</sup> and the focus offset is -15 μm. The dashed lines show ±10 percent control limits for the linewidth. A reticle bias of +1.7 μm was determined by regression analysis.

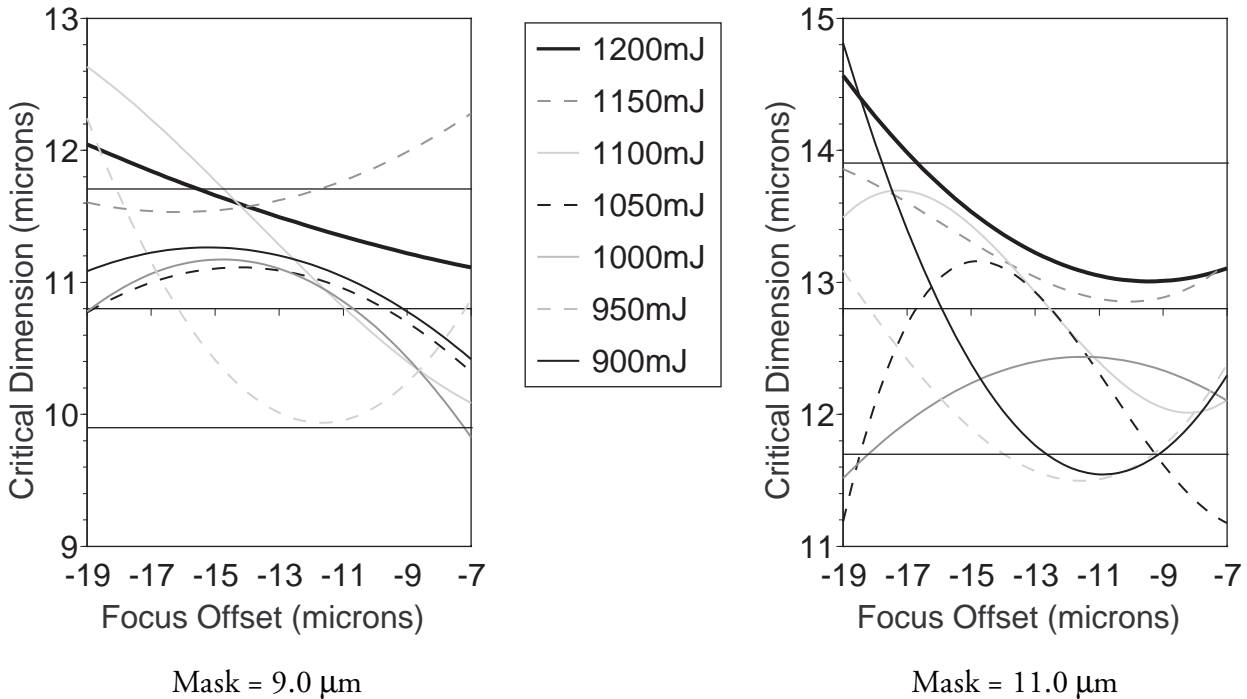


**Figure 3c:** Focus and exposure matrix for Futurrex NR5-8000 photoresist exposed at i-line. The horizontal lines show ±10 percent control limits based on the photomask size. The nominal photoresist size is biased by +1.7 μm based on the photomask linearity.

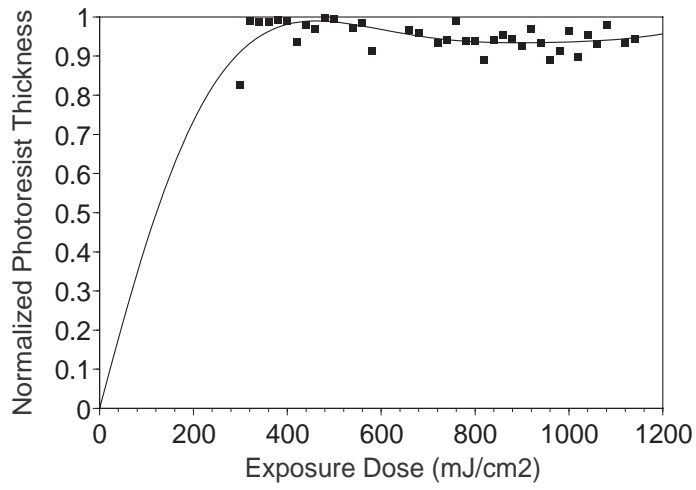


Figure 3d: Photoresist retention plot for Futurrex NR5-8000 at a focus offset of -15  $\mu\text{m}$ .

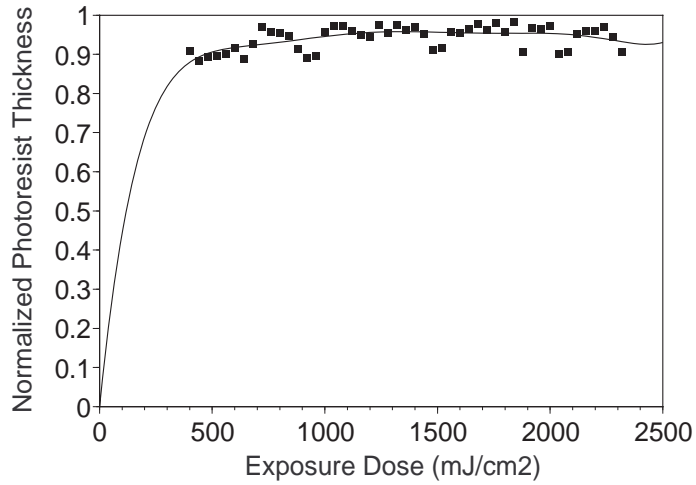


Figure 4d: Photoresist retention plot for JSR THB-30MB at a focus offset of -14  $\mu\text{m}$ .

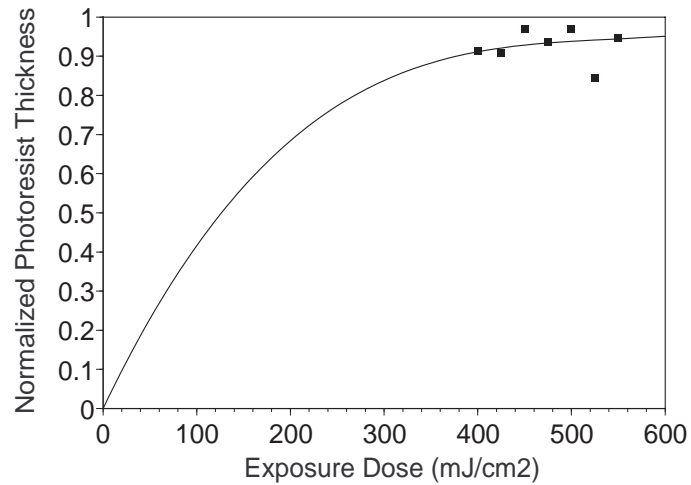
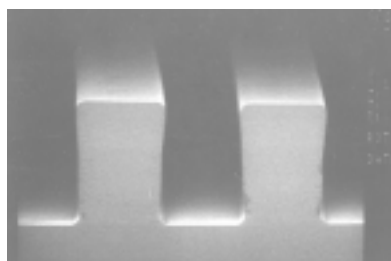
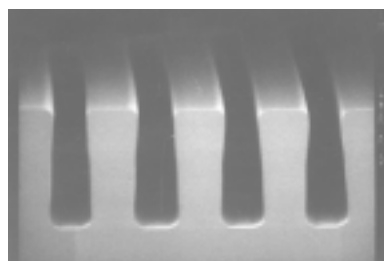


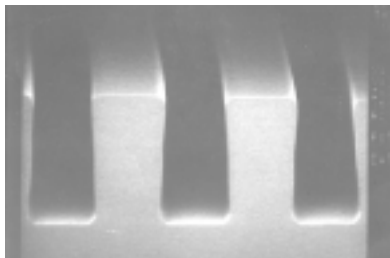
Figure 5d: Photoresist retention plot for MCC SU8-5 at a focus offset of -15  $\mu\text{m}$ .



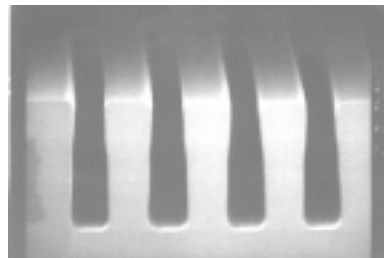
Mask = 30.0  $\mu\text{m}$  line/space



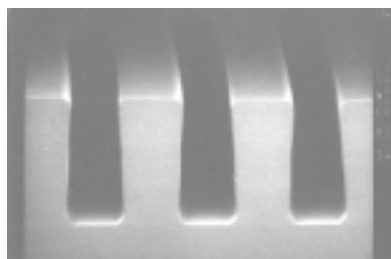
Mask = 15.0  $\mu\text{m}$  line/space



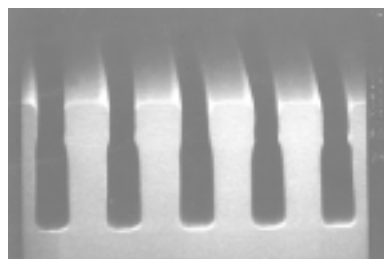
Mask = 24.0  $\mu\text{m}$  line/space



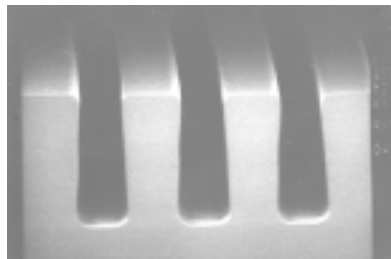
Mask = 14.0  $\mu\text{m}$  line/space



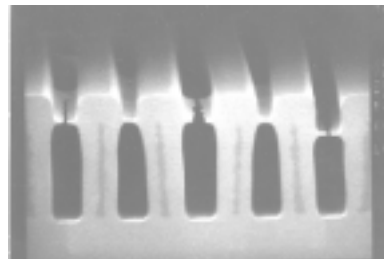
Mask = 20.0  $\mu\text{m}$  line/space



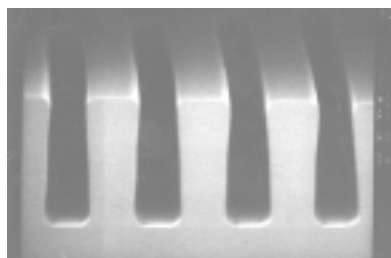
Mask = 13.0  $\mu\text{m}$  line/space



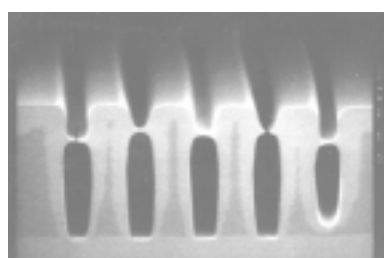
Mask = 18.0  $\mu\text{m}$  line/space



Mask = 12.0  $\mu\text{m}$  line/space

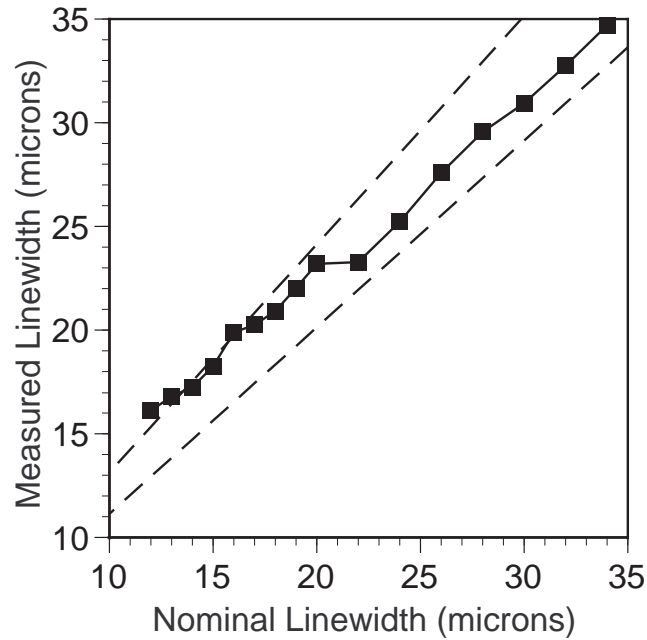


Mask = 16.0  $\mu\text{m}$  line/space

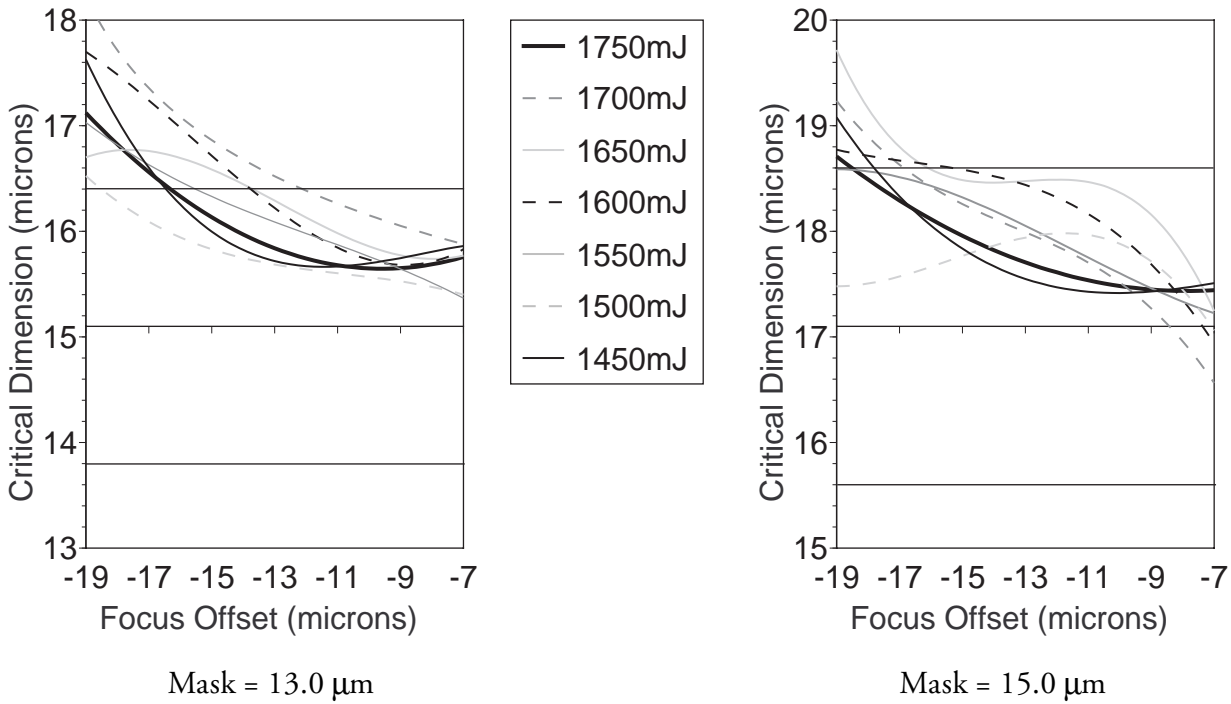


Mask = 11.0  $\mu\text{m}$  line/space

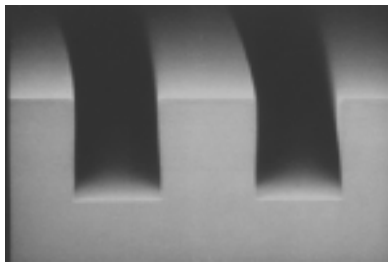
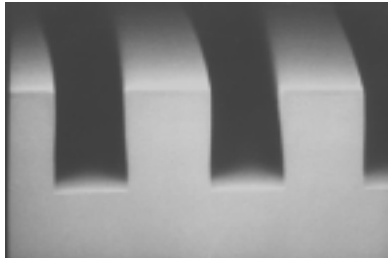
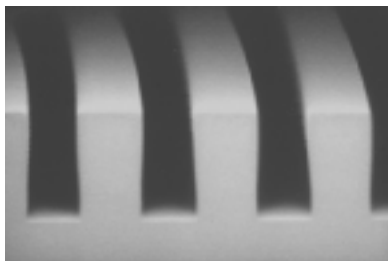
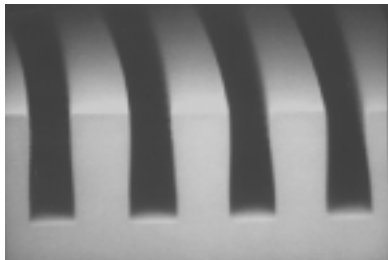
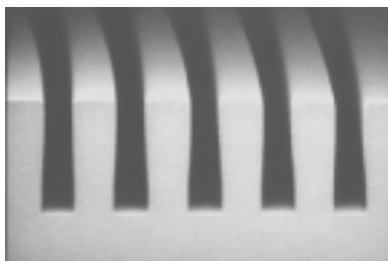
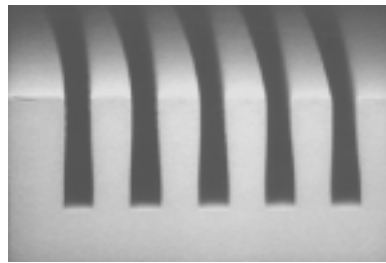
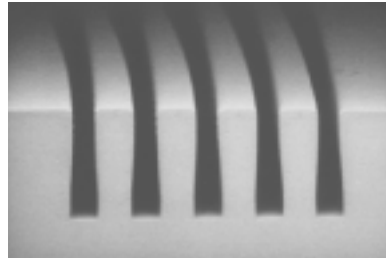
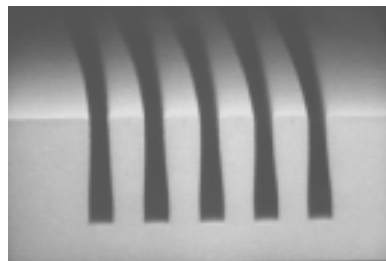
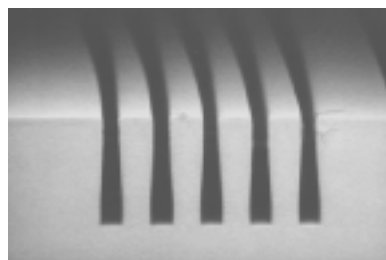
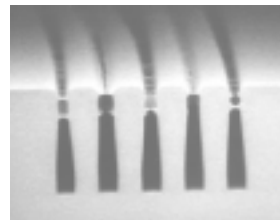
**Figure 4a:** Mask linearity for 50  $\mu\text{m}$  thick JSR THB-30MB photoresist. The exposure dose is 1750  $\text{mJ}/\text{cm}^2$  and the focus offset is -15  $\mu\text{m}$ .



**Figure 4b:** Mask linearity plot for JSR THB-30MB photoresist. The exposure dose is 1750 mJ/cm<sup>2</sup> and the focus offset is -15 μm. The dashed lines show ±10 percent control limits for the linewidth. A reticle bias of +2.1 μm was determined by regression analysis.



**Figure 4c:** Focus and exposure matrix for JSR THB-30MB photoresist exposed at i-line. The horizontal lines show ±10 percent control limits based on the photomask size. The nominal photoresist size is biased by +2.1 μm based on the photomask linearity.

Mask = 30.0  $\mu\text{m}$  line/spaceMask = 26.0  $\mu\text{m}$  line/spaceMask = 18.0  $\mu\text{m}$  line/spaceMask = 16.0  $\mu\text{m}$  line/spaceMask = 12.0  $\mu\text{m}$  line/spaceMask = 11.0  $\mu\text{m}$  line/spaceMask = 10.0  $\mu\text{m}$  line/spaceMask = 9.0  $\mu\text{m}$  line/spaceMask = 8.0  $\mu\text{m}$  line/spaceMask = 7.0  $\mu\text{m}$  line/space

**Figure 5a:** Mask linearity for 50  $\mu\text{m}$  thick MCC SU8-5 photoresist. The exposure dose is 400  $\text{mJ}/\text{cm}^2$  and the focus offset is -9  $\mu\text{m}$ .

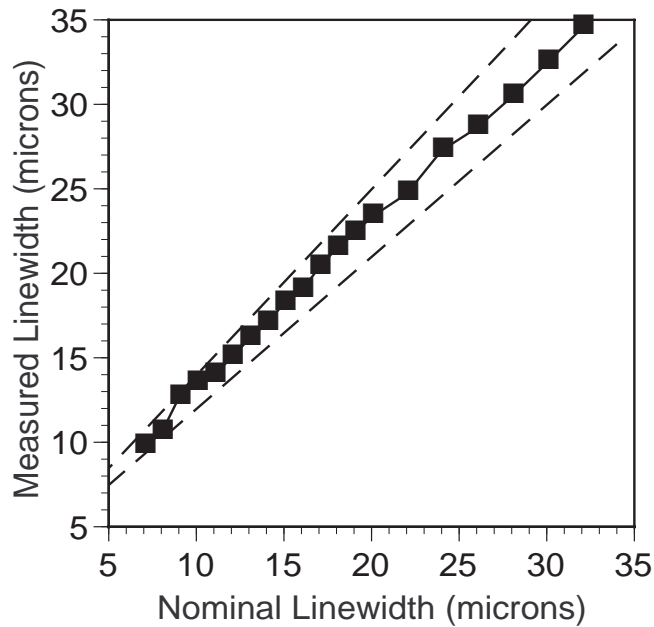


**Figure 5b:** Mask linearity plot for MCC SU8-5 negative photoresist. The exposure dose is  $400 \text{ mJ/cm}^2$  and the focus offset is  $-13 \mu\text{m}$ . The dashed lines show  $\pm 10$  percent control limits for the linewidth. A reticle bias of  $+3.0 \mu\text{m}$  was determined by regression analysis.

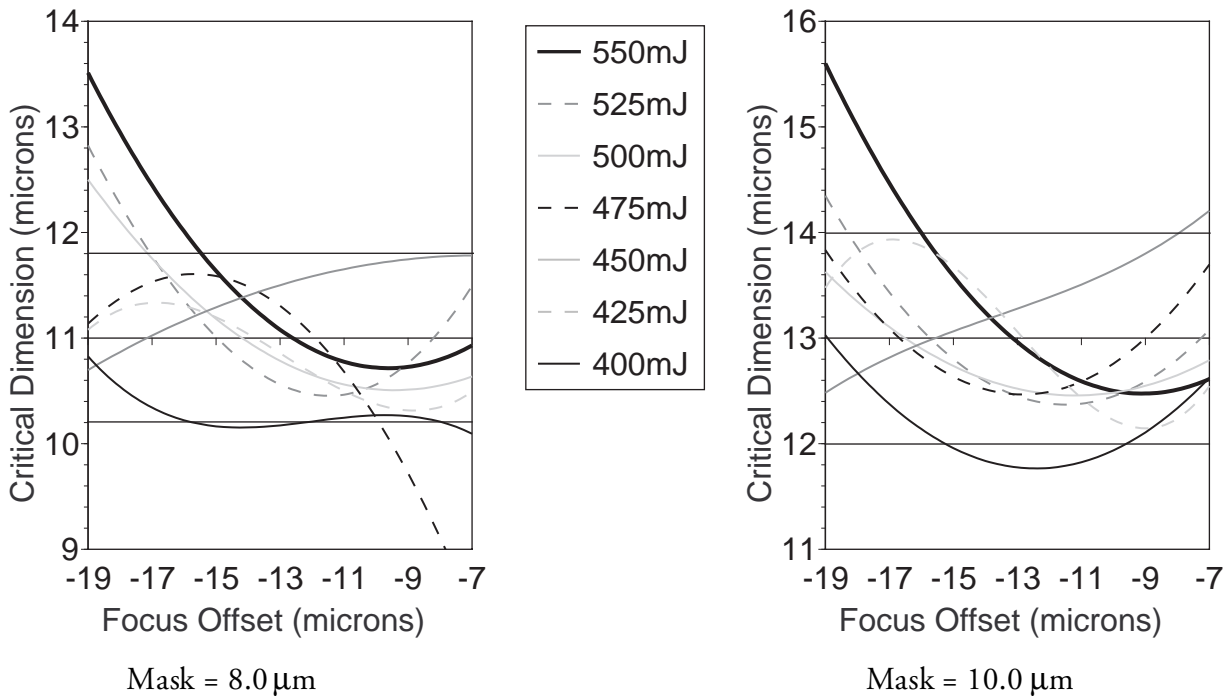


**Figure 5c:** Focus and exposure matrix for MCC SU8-5 photoresist exposed at i-line. The horizontal lines show  $\pm 10$  percent control limits based on the photomask size. The nominal photoresist size is biased by  $+3.0 \mu\text{m}$  based on the photomask linearity.

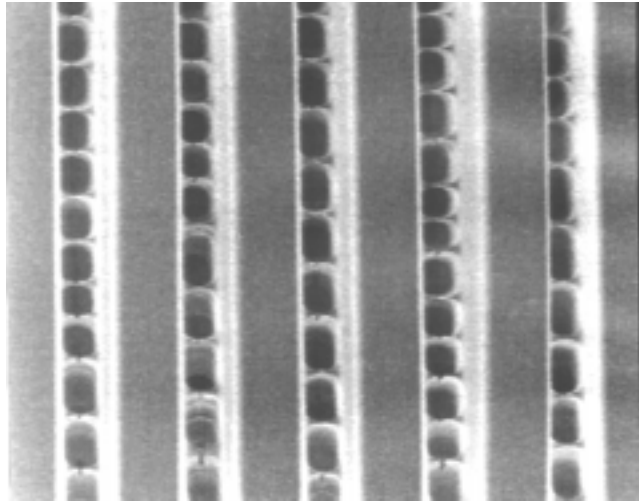


**Figure 6:** Top down image of 7  $\mu\text{m}$  line and space pattern in 50  $\mu\text{m}$  thick MCC SU8-5 photoresist. The exposure dose is 400  $\text{mJ}/\text{cm}^2$  and the focus offset is -9  $\mu\text{m}$ . The observed bubbles are related to the photoresist residue near the top of the film.

Photoresists	AZ-9260	NR5-8000	THB-30MB	MCC SU8-5
Stepper Model	Titan	Saturn	Saturn	Saturn
Resolution ( $\mu\text{m}$ )	11	9	14	8
Nominal Dose ( $\text{mJ}/\text{cm}^2$ )	3050	1100	1750	400
Exposure Latitude ( $\text{mJ}/\text{cm}^2$ )	2800-3100	900-1200	1450-1750	400-550
Focus Latitude ( $\mu\text{m}$ )	-19 to -11	-15 to -7	-17 to -7	-19 to -7
Reticle Bias ( $\mu\text{m}$ )	-2.1	+1.7	+2.1	+3.0

**Table 6:** Recommended lithographic applications on Ultratech steppers in 50  $\mu\text{m}$  films for Clariant AZ-9260, Futurrex NR5-8000, JSR THB-30MB, and MCC SU8-5 photoresists.